HEAT AND MASS TRANSFER ANALYSIS OF MHD MICROPOLAR FLUID IN A CHANNEL WITH CHEMICAL REACTION

Shahzad AHMAD[1], Kashif ALI [2], Muhammad ASHRAF[3]

In this paper, the problem of hydrodynamics micropolar fluid flow in a channel with one wall is shrinking and the other at rest in the presence of chemical reaction including heat and mass transfer characteristics is presented numerically using quasi-linearization method. Effects of some physical parameters on the flow, heat and mass transfer are discussed and presented through tables and graphs.

Keywords: Chemical reaction, heat and mass transfer, shrinking/stationary walls, quasi-linearization.

1. Introduction

The problem of chemical reactions with combined effects of heat and mass transfer has a great importance and therefore has attracted considerable interests of many researchers due its industrial applications such as the manufacturing of ceramics or glassware and polymer production. Hayat et. al. [1] discussed the effects of heat and mass transfer on the magnetohydrodynamic channel flow in the presence of thermal radiation. The hydromagnetic fluid flow in a channel under various situations was studied by Hartmann [2]. Uwanta et al. [3] examined the MHD convection slip fluid flow with radiation and heat deposition in a channel. Rashdan et. al [4] investigated heat and mass fully developed natural convective viscous flow with chemical reaction.

There exist a nonlinear relationship between stress and the rate of strain for non Newtonian fluids, therefore it is very complicated to express all properties of several non Newtonian fluids in a single constitutive equation. Consequently, various non-Newtonian fluid models [(Bachok et. al. [5], Bhadauria and Kiran [6], Abbasbandy et. al.[7], Khandelwal et. al. [8])] have been proposed depending on various physical characters. Micropolar fluid is one of such non-Newtonian fluids, whose equations are highly nonlinear and complicated as compared to those for Newtonian fluids. Hoyt and Fabula [9] predicted experimentally that the non Newtonian fluids display a significant reduction of shear stress and polymeric concentration. The deformation of such materials can be well explained by the theory of micropolar fluids given by Eringen [10,11]. Cheng [12] considered the fully developed natural convection heat and mass transfer of a micropolar fluid in a vertical channel with wall temperatures and concentrations. The micropolar fluid

[1] Bahauddin Zakariya University, Pakistan, email: shahzadahmadbzu@gmail.com
[2] Bahauddin Zakariya University, Pakistan, email: kashifali.381@gmail.com
[3] Bahauddin Zakariya University, pakistan, email: muhammadashraf@bzu.edu.pk

is a hot area of research and therefore many investigators have studied the related problems ([13-18]).

The object of the present study is to investigate the effect of chemical reaction on MHD micropolar fluid flow in a channel with a shrinking and a stationary wall including heat and mass transfer.

2. Mathematical formulation

We now consider hydromagnetic steady laminar viscous flow with heat and mass transfer of an incompressible micropolar fluid in a parallel plate channel with lower wall shrinking and the upper at rest, under the influence of chemical reaction and transverse applied magnetic field as shown in Fig. 1. The induced magnetic field is assumed to be negligible as compared with the imposed field. The magnetic Reynolds number, which used to compare the transport of magnetic lines of force in a conducting fluid with the leakage of such lines from the fluid, is assumed to be small. Moreover, no applied polarization and hence no electric field. The body couple is absent. The two walls of the channel are located at $y = \pm d$. The velocity (u, v, w) and microrotation $(\upsilon_1, \upsilon_2, \upsilon_3)$ field may be expressed as

$$u = u(x, y), v = v(x, y), w = 0, \upsilon_1 = 0, \upsilon_2 = 0, \upsilon_3 = N(x, y), \tag{1}$$

where N is the component of the microrotation normal to the $xy-$plane.

The governing equations for the problem are,

$$\frac{\partial u}{\partial x} + \frac{\partial v}{\partial y} = 0, \tag{2}$$

$$u\frac{\partial u}{\partial x} + v\frac{\partial u}{\partial y} = \frac{-1}{\rho}\frac{\partial p}{\partial x} + \frac{(\mu + \kappa)}{\rho}\nabla^2 u + \frac{\kappa}{\rho}\frac{\partial N}{\partial y} - \frac{\sigma {B_0}^2}{\rho}u, \tag{3}$$

$$u\frac{\partial v}{\partial x} + v\frac{\partial v}{\partial y} = \frac{-1}{\rho}\frac{\partial p}{\partial y} + \frac{(\mu + \kappa)}{\rho}\nabla^2 v - \frac{\kappa}{\rho}\frac{\partial N}{\partial x}, \tag{4}$$

$$\rho j(u\frac{\partial N}{\partial x} + v\frac{\partial N}{\partial y}) = \gamma_1 \nabla^2 N + \kappa(\frac{\partial v}{\partial x} - \frac{\partial u}{\partial y}) - 2\kappa N, \tag{5}$$

$$\rho c_p \left(u\frac{\partial T}{\partial x} + v\frac{\partial T}{\partial y} \right) = k_0 \frac{\partial^2 T}{\partial y^2}, \tag{6}$$

$$u\frac{\partial C}{\partial x} + v\frac{\partial C}{\partial y} = D\frac{\partial^2 C}{\partial y^2} - K(C - C_2), \tag{7}$$

where ρ is the density, p is the pressure, μ is the dynamic viscosity, κ is the vortex viscosity, σ is the electrical conductivity, B_0 is the strength of the magnetic field, j is the micro-inertia density, γ_1 is the spin gradient viscosity, c_p

is the specific heat at constant pressure, κ_0 is the thermal conductivity, T is the temperature of the fluid, C is the concentration, D is the mass diffusivity and K is the rate of chemical reaction.

The boundary conditions for the present problem are

$$\left.\begin{aligned} &u(x,-d) = -U = -bx, u(x,d) = 0, v(x,\pm d) = 0, N(x,\pm d) = 0, \\ &T(x,-d) = T_1, T(x,d) = T_2,\ C(x,-d) = C_1,\ C(x,d) = C_2, \end{aligned}\right\} \tag{8}$$

where $b > 0$ is the shrinking rate of the channel walls, T_1 and T_2 (with $T_1 > T_2$) are the fixed temperatures and C_1 and C_2 are the fixed concentrations of the lower and upper channel respectively.

The partial differential Equations $(2)-(7)$ can be converted into ordinary differential equations by using the following similarity transformations,

$$\eta = \frac{y}{d}, u = bxf'(\eta), v = -dbf(\eta), N = -\frac{b}{d}xg(\eta), \theta(\eta) = \frac{T-T_2}{T_1-T_2}, \chi(\eta) = \frac{C-C_2}{C_1-C_2}. \tag{9}$$

The velocity components given in Equation (9) satisfy the continuity Equation (2) and hence represent a possible fluid motion.

After eliminating the pressure term from Equations (3) and (4), we introduce the above similarity transformation to the resulting equation to get,

$$(1+C_1)f^{iv} - C_1 g'' = R(ff'' - ff''') + Mf'', \tag{10}$$

where as Equations $(5)-(7)$, in view of Equation (9), are

$$C_3 g'' + C_1 C_2 (f'' - 2g) = f'g - fg', \tag{11}$$

$$\theta'' + \Pr R\, f\theta' = 0. \tag{12}$$

$$\chi'' + RSc\chi' - Sc\gamma\chi = 0, \tag{13}$$

Here $C_1 = \frac{\kappa}{\mu}$ is the vortex viscosity parameter, $C_2 = \frac{\mu}{\rho jb}$ is the microinertia density parameter, $C_3 = \frac{\gamma_1}{\rho jd^2 b}$ is the spin gradient viscosity parameter, $R = \frac{\rho d^2 b}{\mu}$ is the shrinking Reynolds number, $M = \frac{d^2 \sigma B_0^{\,2}}{\mu}$ is the magnetic parameter, $\Pr = \frac{\mu c_p}{\kappa_0}$ is the Prandtl number, $Sc = \upsilon / D$ is the Schmidt number and $\gamma = \frac{Kd^2}{\upsilon}$ is the chemical reaction parameter.

It is worth mentioning that, in the present study, we have considered the mass transfer of a chemically reactive species in the channel. Micropolar fluid inside the channel is assumed to contain some chemically reactive species, and the

mixture thus formed is homogeneous. Moreover, 1st order homogeneous and irreversible reaction is assumed to be taking place in the fluid because of chemical reactive nature of the species. Further, in Equation (7), the reaction rate constant K is the measure how fast the chemical reaction is taking place in the fluid inside the channel. It is to note that the negative term on the right hand side of the equation shows that the chemical reaction taking place in the fluid is destroying the species. Finally, the reaction rate constant K is combined with the material property υ and the geometric dimension d, to give rise to the chemical reaction parameter $\gamma\left(=\frac{Kd^2}{\upsilon}\right)$.The traditional way (Ali *et al.* [19]) of studying the fluid dynamics problems is to specify the values of these dimensionless parameters rather than specifying the particular fluid properties and the domain dimensions. Boundary conditions given in Equation (8) in view of similarity transformations given in Equation (9) can be written as,

$$f(\pm 1)=0,\ f'(-1)=-1,\ f'(1)=0,\ g(\pm 1)=0, \theta(-1)=1, \theta(1)=0. \tag{14}$$

3. Numerical solution using Quasi-linearization method

In quasi-linearization, we construct the sequences of vectors $\left\{f^{(k)}\right\},\left\{g^{(k)}\right\},\left\{\theta^{(k)}\right\},\left\{\chi^{(k)}\right\}$ which converge to the numerical solutions of Equations $(10),(11),(12)$ and (13) respectively. To construct $\left\{f^{(k)}\right\}$ we linearize Equation (10), by retaining only the first order terms, as follows:

We set: $G(f, f', f'', f''', f^{iv}) \equiv (1+C_1) f^{iv} + Rff''' - Rf f'' - Mf'' - C_1 g'',$

$$G(f^{(k)}, f^{(k)'}, f^{(k)''}, f^{(k)''}, f^{(k)iv}) + \left(f^{(k+1)} - f^{(k)}\right)\frac{\partial G}{\partial f^{(k)}} + \left(f^{(k+1)'} - f^{(k)'}\right)\frac{\partial G}{\partial f^{(k)'}} +$$

$$\left(f^{(k+1)''} - f^{(k)''}\right)\frac{\partial G}{\partial f^{(k)''}} + \left(f^{(k+1)'''} - f^{(k)'''}\right)\frac{\partial G}{\partial f^{(k)'''}} + \left(f^{(k+1)iv} - f^{(k)iv}\right)\frac{\partial G}{\partial f^{(k)iv}} = 0,$$

which simplifies to:

$$\left.\begin{aligned}&(1+C_1) f^{(k+1)iv} + Rf^{(k)} f^{(k+1)'''} - \left(Rf^{(k)'} + M\right) f^{(k+1)''} - Rf^{(k)''} f^{(k+1)'} + \\ &Rf^{(k)'''} f^{(k+1)} = R\left(-f^{(k)'} f^{(k)''} + f^{(k)} f^{(k)'''}\right) + C_1 g^{(k)''}.\end{aligned}\right] \tag{15}$$

Now Equation (15) gives a system of linear differential equations with f^k being the numerical solution vector of the k^{th} equation. To solve the ODEs, we replace

the derivatives with their central difference approximations, giving rise to the sequence $\left\{ f^{(k)} \right\}$, generated by the following linear system:

$$Af^{(k+1)} = B \text{ with } A = A\left(f^{(k)}\right) \text{ and } B = B\left(f^{(k)}, g^{(k)}\right), \tag{16}$$

where n is the number of grid points. The matrices A_{nxn} and B_{nx1} are initialized as follows:

$$A_{1,1} = 1, B_1 = 0,$$

$$A_{2,1} = \left(-4(1+\mathrm{C}_1) + hRf_1 - Mh^2\right), A_{2,2} = \left(7(1+C_1) - hRf_2 + h^2R\alpha + \frac{hR}{2} f_4 + 2Mh^2\right),$$

$$A_{2,3} = \left(-4(1+\mathrm{C}_1) - hRf_3 - Mh^2\right), A_{2,4} = \left((1+\mathrm{C}_1) + \frac{hR}{2} f_2\right),$$

$$B_2 = \begin{pmatrix} h^2C_1(g_3 - 2g_2 + g_1) + \frac{hR}{2} f_2(-f_2 + 2f_1 - 2f_3 + f_4) \\ -\frac{hR}{2}(f_3 - f_1)(f_3 - 2f_2 + f_1) + 2h\alpha(1+C_1) \end{pmatrix},$$

$$\left.\begin{aligned} &A_{i,i-2} = \left((1+\mathrm{C}_1) - \frac{hR}{2} f_i\right), A_{i,i-1} = \left(-4(1+C_1) + hRf_{i-1} - Mh^2\right), \\ &A_{i,i} = \left(6(1+\mathrm{C}_1) + \frac{hR}{2}(f_{i+2} - f_{i-2}) + 2Mh^2\right), \\ &A_{i,i+1} = \left(-4(1+C_1) - hRf_{i+1} - Mh^2\right), A_{i,i+2} = \left((1+\mathrm{C}_1) + \frac{hR}{2} f_i\right), \\ &B_i = \left(h^2C_1(g_{i+1} - 2g_i + g_{i-1}) + \frac{hR}{2} f_i(-f_{i-2} + 2f_{i-1} - 2f_{i+1} + f_{i+2}) - \frac{hR}{2}(f_{i+1} - f_{i-1})(f_{i+1} - 2f_i + f_{i-1})\right), \end{aligned}\right\} 2 < i < (n-1)$$

$$\left.\begin{aligned} &A_{n-1,n-3} = \left((1+\mathrm{C}_1) - \frac{hR}{2} f_{n-1}\right), A_{n-1,n-2} = \left(-4(1+C_1) + hRf_{n-2} - Mh^2\right), \\ &A_{n-1,n-1} = \left(6(1+\mathrm{C}_1) + \frac{hR}{2}(f_{i+2} - f_{i-2}) + 2Mh^2\right), A_{n-1,n} = \left(-4(1+C_1) - hRf_{i+1} - Mh^2\right), \\ &B_{n-1} = \begin{pmatrix} h^2C_1(g_{i+1} - 2g_i + g_{i-1}) + \frac{hR}{2} f_i(-f_{i-2} + 2f_{i-1} - 2f_{i+1} + f_{i+2}) \\ -\frac{hR}{2}(f_{i+1} - f_{i-1})(f_{i+1} - 2f_i + f_{i-1}) \end{pmatrix}, \\ &A_{n,n} = 1, B_n = 0. \end{aligned}\right\} \tag{17}$$

(The superscripts have been dropped for simplicity & clarity)

On the other hand, Equations (11), (12) and (13) are linear in $g, \theta \& \chi$ respectively. Therefore, in order to generate the sequences $\left\{g^{(k)}\right\}, \left\{\theta^{(k)}\right\} \& \left\{\chi^{(k)}\right\}$ these equations may be written as

$$C_3 g^{(k+1)''} + C_1 C_2 (f^{(k+1)''} - 2g^{(k+1)}) = f^{(k+1)'} g^{(k+1)} - f^{(k+1)} g^{(k+1)'}, \tag{18}$$

$$\theta^{(k+1)''} + \Pr R f^{(k+1)} \theta^{(k+1)'} = 0. \tag{19}$$

$$\chi^{(k+1)''} + R\, Sc\, \chi^{(k+1)'} - Sc\, \gamma\, \chi^{(k+1)} = 0, \tag{20}$$

Importantly $f^{(k+1)}$ is considered to be known in the above equations. We outline the computational procedure as follows:

- Provide the initial guess $f^{(0)}, g^{(0)}, \theta^{(0)} \& \chi^{(0)}$, satisfying the boundary conditions given in Equation (14)
- Solve the linear system given by Equation (16) to find $f^{(1)}$
- Use $f^{(1)}$ to solve the linear system arising from the FD discritization of Equations (18), (19) and (20), to get $g^{(1)}, \theta^{(1)} \& \chi^{(1)}$.
- Take $f^{(1)}, g^{(1)}, \theta^{(1)} \& \chi^{(1)}$ as the new initial guesses & repeat the procedure to generate the sequences $\left\{f^{(k)}\right\}, \left\{g^{(k)}\right\}, \left\{\theta^{(k)}\right\} \& \left\{\chi^{(k)}\right\}$ which, respectively, converge to $f, g, \theta \& \chi$ (the numerical solutions of Equations (10), (11), (12) and (13)).
- The three sequences are generated until

$$max\left\{\left\|f^{(k+1)} - f^{(k)}\right\|_{L_\infty}, \left\|g^{(k+1)} - g^{(k)}\right\|_{L_\infty}, \left\|\theta^{(k+1)} - \theta^{(k)}\right\|_{L_\infty}, \left\|\chi^{(k+1)} - \chi^{(k)}\right\|_{L_\infty}\right\} < 10^{-6}.$$

The matrix A (in Equation (17)) is pentadiagonal & not diagonally dominant, and hence the SOR method may fail or work very poorly. Therefore, some direct method like LU factorization or Guassian elimination with full pivoting (to ensure stability) may be employed.

We may improve the order of accuracy of the solution by solving the problem again on the grid with step $h/2$ & $h/4$, and then using the Richardson extrapolation which have been carried out at not only the common grid points but also at the skipped points, by following Roache and Knupp [20]. Any extrapolation scheme (Deuflhard [21]) may be used for this purpose but we have used the polynomial extrapolation.

4. Results and discussion

The physical quantities of our interest are the shear stress, the couple stress, the heat transfer rate and
the mass transfer rate at the channel walls which are, respectively, proportional to the values of f'', g', θ' and χ' at the walls. The parameters of the study are the magnetic parameter M, the shrinking Reynolds number R, the micropolar parameters C_1, C_2 and C_3, the Prandtl number Pr, the Schmidt number Sc and the chemical reaction parameter γ. We shall study the effects of the parameters on $f''(\pm 1), g'(\pm 1)$, $\theta'(\pm 1)$ and $\chi'(\pm 1)$, as well as, on the velocity profiles $f(\eta), f'(\eta)$, the microrotation profile $g(\eta)$, the heat profile $\theta(\eta)$ and the concentration profile $\chi(\eta)$.

The values of the micropolar parameters C_1, C_2 & C_3 are given in Table 1, whereas the case 1 corresponds to the Newtonian fluid. In order to study their effect on different aspects of the problem, they are arbitrarily chosen, as done customarily in the works of many researchers (for example, Ashraf *et al.* [13, 14] and Ali *et al.* [22, 23] etc).

Table 1

Five cases of values of micropolar parameters C_1, C_2 and C_3.

Cases	C_1	C_2	C_3
1(Newtonian)	0	0	0
2	2	0.3	0.2
3	4	0.6	0.4
4	6	0.9	0.6
5	8	1.2	0.8

Table 2 shows the convergence of our numerical results as the step-size decreases which gives us confidence on our computational procedure. Table 3 shows that external magnetic increases the shear stress at the shrinking wall. This is because the external magnetic field exerts a force, called the Lorentz force, which tends to drag the fluid towards the shrinking wall, which causes greater spinning of the micro fluid particles, and hence increases the couple stress as well. Moreover, the frictional force raises the temperature of the fluid, therefore, the heat transfer rate at the shrinking wall only, which is directly proportional to the temperature difference also increases while mass transfer increases at the shrinking wall and decreases at the other wall.

It is clear from the Table 4 that the shear and couple stresses as well as the heat transfer rate at the shrinking wall may decrease as the Reynolds number increases. The increased shrinking rate of the wall forces the fluid to move rapidly away

from the shrinking wall, thus decreasing both the shear and couple stresses. Also, the fluid carries away heat from the region near the lower wall, thus decreasing the temperature difference and hence the heat transfer rate at the shrinking wall. On theother hand, the incoming of the heated fluid towards the upper wall increases not only the shear and couple stresses but also the heat transfer rate.

Table 2

Dimensionless temperature $\theta(\eta)$ on three grid sizes and extrapolated values for $C_1 = 4, C_2 = 0.6, C_3 = 0.4, R = 10, M = 10$ and $Pr = 0.5$.

	$\theta(\eta)$			
η	1st grid ($h = 0.02$)	2nd grid ($h = 0.01$)	3rd grid ($h = 0.005$)	Extrapolated values
-0.8	0.968141	0.968135	0.968133	0.968133
-0.4	0.882378	0.882360	0.882356	0.882354
0	0.730568	0.730542	0.730535	0.730533
0.4	0.483994	0.483972	0.483966	0.483964
0.8	0.167010	0.167003	0.167002	0.167001

Table 3

The effect of magnetic field on shear and couple stresses, heat transfer rate and concentration with $R = 10, C_1 = 4, C_2 = 0.6, C_3 = 0.4, \gamma = 1, Sc = 1$ and $Pr = 0.5$.

M	$f''(-1)$	$g'(-1)$	$\theta'(-1)$	$\chi'(-1)$
0	1.238012	2.365594	-0.124255	-0.442033
4	1.478036	2.519487	-0.137260	-0.453635
8	1.697361	2.651646	-0.149030	-0.464600
12	1.899491	2.766694	-0.159704	-0.474944
16	2.087179	2.868030	-0.169415	-0.484698
M	$f''(1)$	$g'(1)$	$\theta'(1)$	$\chi'(1)$
0	-1.182668	1.201500	-0.903785	-0.802913
4	-1.083242	1.097535	-0.873035	-0.763852
8	-1.005609	1.013123	-0.847501	-0.731176
12	-0.943843	0.943407	-0.825990	-0.703479
16	-0.893884	0.884959	-0.807634	-0.679721

Table 4

The effect of stretching Reynolds number on shear and couple stresses and heat transfer rate and concentration with $M = 15, C_1 = 4, C_2 = 0.6, C_3 = 0.4, \gamma = 1, Sc = 1$ and $Pr = 0.5$.

R	$f''(-1)$	$g'(-1)$	$\theta'(-1)$	$\chi'(-1)$
0	2.345599	3.000168	-0.500000	-1.037277
6	2.164237	2.908497	-0.272958	-0.637753
12	1.979722	2.810449	-0.127150	-0.429553
18	1.793832	2.706345	-0.050061	-0.330915
24	1.609153	2.597096	-0.016617	-0.277711

R	$f''(1)$	$g'(1)$	$\theta'(1)$	$\chi'(1)$
0	-0.758610	0.787158	-0.500000	-0.275713
6	-0.842175	0.851331	-0.681539	-0.509844
12	-0.939585	0.923788	-0.878121	-0.773331
18	-1.053067	1.005305	-1.074517	-1.028990
24	-1.184668	1.096294	-1.262613	-1.270988

From Table 5, the micropolar structure of the fluid tends to reduce the shear stress at the walls, which is in accordance with the experimental prediction of Hoyt and Fabula [9] that the micro fluid particles cause significant reduction in shear stress near a rigid body. Moreover, the particles also cause the microrotation in the fluid which is responsible for the couple stress at the two channel walls. The micropolar parameters also tend to raise the heat and mass transfer rate at the stationary wall while decreasing at the shrinking wall. It is clear from Table 6 that the Prandtl number reduces the heat transfer at the shrinking wall and an opposite effect is noted at the other wall. The increase of Schmidt number and chemical parameter result in increasing the mass transfer rate at the shrinking wall (see Tables 7 & 8).

Table 5

The effect of micropolar coefficients on shear and couple stresses, heat transfer rate and concentration with $M = 10, R = 10, \gamma = 1, Sc = 1$ and $Pr = 0.5$.

Cases	$f''(-1)$	$g'(-1)$	$\theta'(-1)$	$\chi'(-1)$
1	3.417152	0	-0.223950	-0.508879
2	2.403962	1.807868	-0.180259	-0.478901
3	2.041483	2.711074	-0.167071	-0.469848
4	1.846625	3.364088	-0.161031	-0.465765
5	1.723257	3.891092	-0.157674	-0.463546
Cases	$f''(1)$	$g'(1)$	$\theta'(1)$	$\chi'(1)$
1	-1.097206	0	-0.729532	-0.648764
2	-1.046426	0.468183	-0.792992	-0.704165
3	-0.973031	0.976669	-0.811966	-0.716777
4	-0.914918	1.363344	-0.820081	-0.720535
5	-0.871144	1.672673	-0.824319	-0.721720

Table 6

Effect of Prandtl number on heat transfer rate with $M = 15, R = 5, C_1 = 4, C_2 = 0.6, C_3 = 0.4,$ $\gamma = 1, Sc = 1$

Pr	$\theta'(-1)$	$\theta'(1)$
0.2	-0.413670	-0.559694
0.6	-0.274365	-0.679543
1.0	-0.175383	-0.795188
1.4	-0.108779	-0.902861
1.8	-0.065881	-1.000986

Table 7

Effect of the Schmidt number on mass transfer with $M = 10, R = 5, C_1 = 4, C_2 = 0.6, C_3 = 0.4,$ $\gamma = 1.5, Pr = 0.5$

Sc	$\chi'(-1)$	$\chi'(1)$
0	-0.500000	-0.500000
0.4	-0.678801	-0.440020
0.8	-0.821402	-0.397659
1.2	-0.942528	-0.365638
1.6	-1.049452	-0.340251

Table 8

Effect of the chemical parameter on mass transfer with

$M = 10, R = 5, C_1 = 4, C_2 = 0.6, C_3 = 0.4, \quad Sc = 1.0, Pr = 0.5$

γ	$\chi'(-1)$	$\chi'(1)$
0	-0.163615	-0.816441
0.3	-0.335974	-0.690269
0.6	-0.491172	-0.588715
0.9	-0.632672	-0.505884
1.2	-0.763010	-0.437557

The streamlines for the present problem are shown in Fig. 2, which show that the fluid is moving with higher velocity near the shrinking wall (as the streamlines are closer), which makes sense due to the no slip condition.

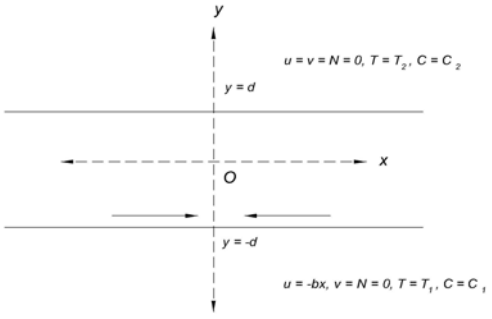

Fig. 1. Physical Configuration

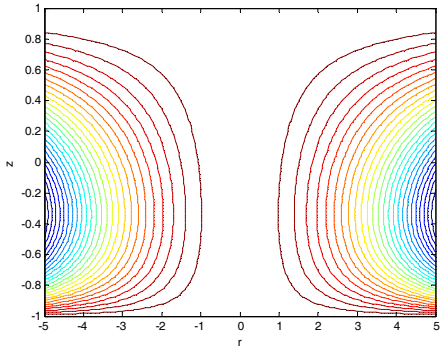

Fig. 2. Streamlines for the problem for $C_1 = 4, C_2 = 0.6, C_3 = 0.4, R = 10$ and $M = 10$

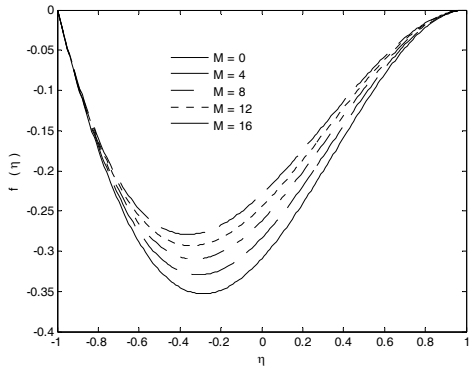

Fig. 3. Normal velocity profiles for $R = 10, C_1 = 4,$ $C_2 = 0.6,\ C_3 = 0.4,\ \gamma = 1, Sc = 1, Pr = 0.5$ and various M

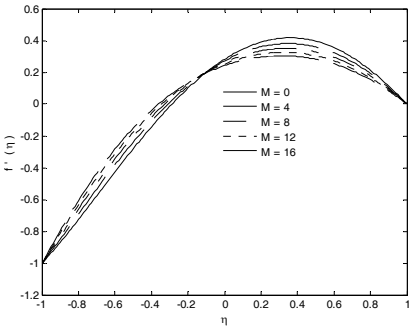

Fig. 4. Streamwise velocity profiles for $R = 10, C_1 = 4,\ C_2 = 0.6, C_3 = 0.4,\ \gamma = 1,$ $Sc = 1, Pr = 0.5$ and various M

The magnetic parameter M not only reduces the two velocities but also the temperature and concentration profiles across the whole channel whereas it raises the microrotation distribution only in a smaller region near a shrinking wall (Figures 3-7).

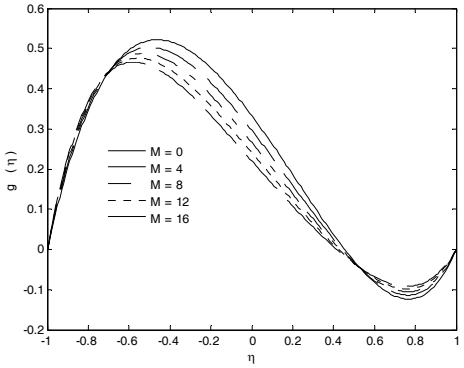

Fig. 5. Microrotation profiles for $R = 10, C_1 = 4,$ $C_2 = 0.6,\ C_3 = 0.4,\ \gamma = 1, Sc = 1, Pr = 0.5$ and various M

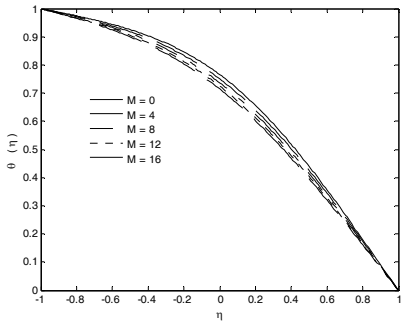

Fig. 6. Temperature profiles for $R = 10, C_1 = 4, C_2 = 0.6,$ $C_3 = 0.4,\ \gamma = 1, Sc = 1, Pr = 0.5$ and various M

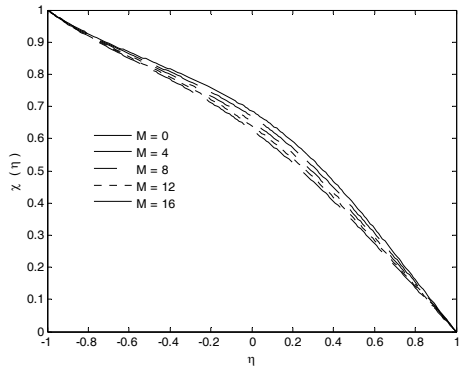

Fig. 7. Concentration profiles for $R = 10, C_1 = 4,$ $C_2 = 0.6,\ C_3 = 0.4,\ \gamma = 1, Sc = 1, Pr = 0.5$ and various M

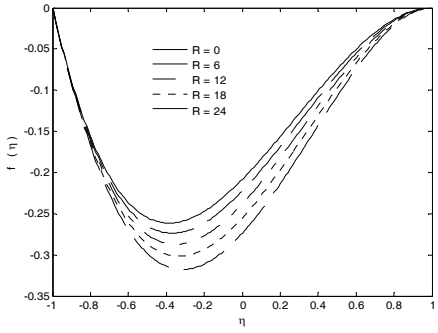

Fig. 8. Normal velocity profiles for $M = 15, C_1 = 4,\ C_2 = 0.6, C_3 = 0.4, \gamma = 1,$ $Sc = 1, Pr = 0.5$ and various R

The effect of the shrinking Reynolds number R on the different profiles is opposite to that of M (Figs. 8-12). It is observe from the Figs. 13-17 that the micropolar parameters increase the velocities, microrotation, temperature and concentration profiles across the whole domain.

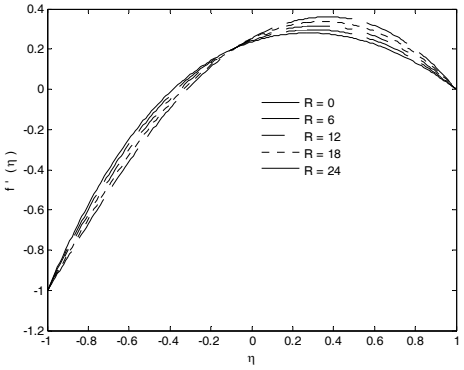

Fig. 9. Streamwise velocity profiles for $M = 15,$ $C_1 = 4,\ C_2 = 0.6, C_3 = 0.4, \gamma = 1, Sc = 1, Pr = 0.5$ and various R

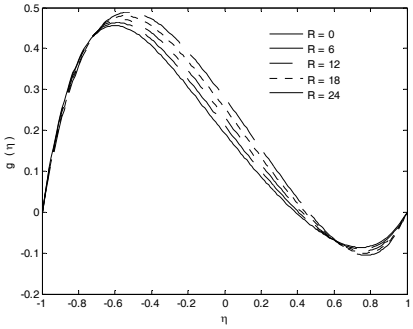

Fig. 10. Microrotation profiles for $M = 15, C_1 = 4,\ C_2 = 0.6,$ $C_3 = 0.4, \gamma = 1, Sc = 1, Pr = 0.5$ and various R

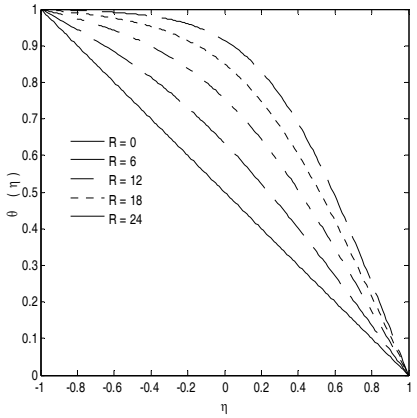

Fig. 11. Temperature profiles for $M = 15, C_1 = 4,$ $C_2 = 0.6,\ C_3 = 0.4, \gamma = 1, Sc = 1, Pr = 0.5$ and various R

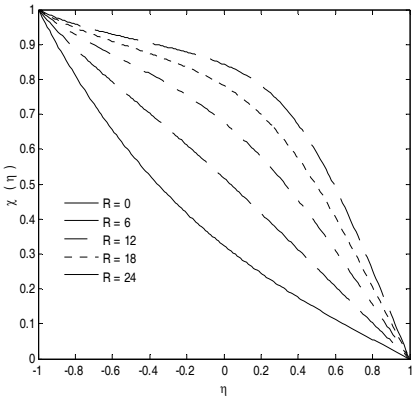

Fig. 12. Concentration profiles $M = 15, C_1 = 4, C_2 = 0.6,$ $C_3 = 0.4, \gamma = 1, Sc = 1, Pr = 0.5$ and various R

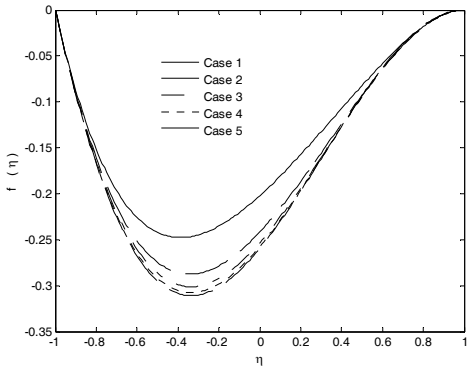

Fig. 13. Normal velocity profiles for $R = 10, M = 10, \gamma = 1, Sc = 1, Pr = 0.5$ and various cases of the micropolar parameters

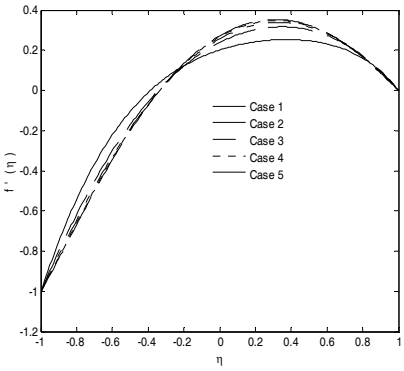

Fig. 14. Streamwise velocity profiles for $R = 10, M = 10, \gamma = 1, Sc = 1, Pr = 0.5$ and various cases of the micropolar parameters

Fig. 18 shows that the influence of the Prandtl number on the heat profile is similar to that of R.

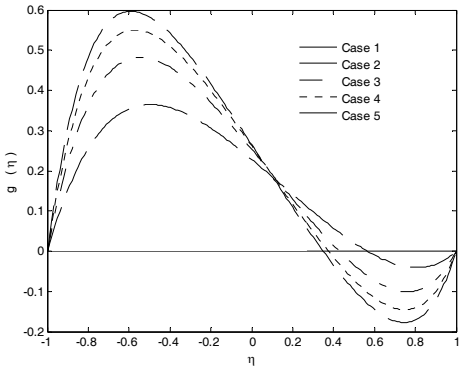

Fig. 15. Microrotation profiles for $R = 10, M = 10, \gamma = 1, Sc = 1, Pr = 0.5$ and various cases of the micropolar parameters

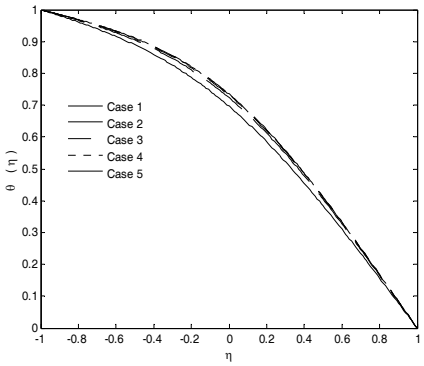

Fig. 16. Temperature profiles for $R = 10, M = 10, \gamma = 1, Sc = 1, Pr = 0.5$ and various cases of the micropolar parameters

The influence of the Schmidt number *Sc* is to lower the concentration profile as shown in Figure 19. Finally, the effect of the chemical reaction parameter on the concentration distribution is similar to that of Schmidt number (Figure 20).

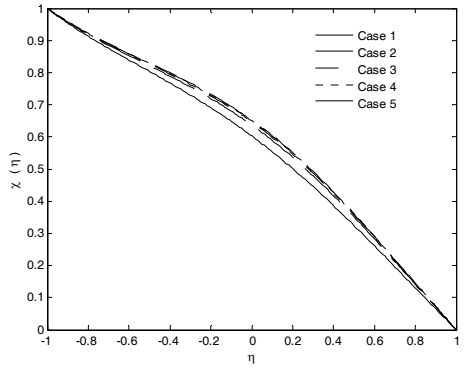

Fig. 17. Concentration profiles for $R = 10, M = 10, \gamma = 1, Sc = 1, Pr = 0.5$ and various cases of the micropolar parameters

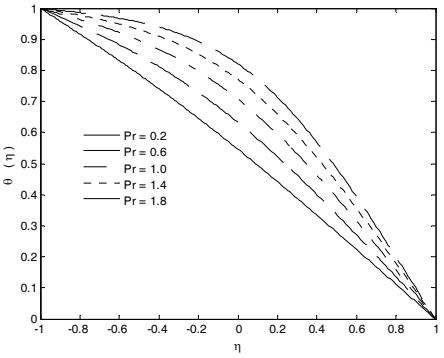

Fig. 18. Temperature profiles for $M = 15, R = 5, C_1 = 4, C_2 = 0.6, C_3 = 0.4, \gamma = 1, Sc = 1$ and various Pr

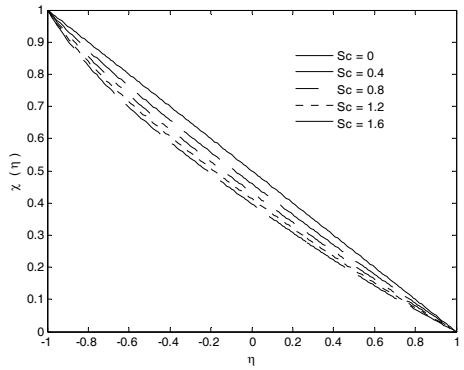

Fig. 19. Concentration profiles for $M = 10, R = 5, C_1 = 4,\ C_2 = 0.6, C_3 = 0.4,$ $\gamma = 1.5, Pr = 0.5$ and various Sc

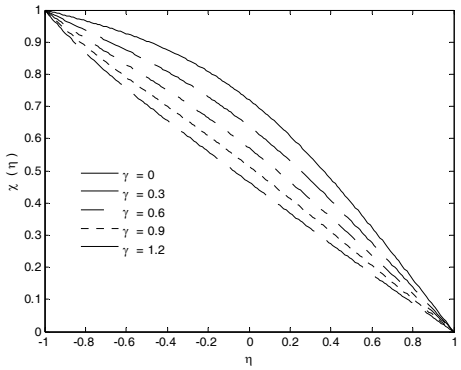

Fig. 20. Concentration profiles for $M = 10, R = 5, C_1 = 4,\ C_2 = 0.6, C_3 = 0.4,$ $Sc = 1.0, Pr = 0.5$ and various γ

5. Conclusions

We have numerically studied the problem of a viscous incompressible electrically conducting micropolar fluid in a channel with one wall shrinking and the other at rest. It has been observed that the external magnetic field tends to reduce the velocities, temperature and concentration distributions across the whole domain channel while it raises the microrotation distribution only in a smaller region near a shrinking wall. The micropolar fluid exhibit significant reduction in the shear stress at the channel walls. The mass concentration and chemical reaction raise the mass transfer at the shrinking wall.

Acknowledgements

The authors are extremely grateful to the Higher Education Commission of Pakistan for the financial support to carry out this research. The authors are also very grateful to the learned reviewer for the useful comments improving the quality of the paper.

R E F E R E N C E S

[1] *T.Hayat, M.Awais, A.Alsaedi and A.Safdar,* "On Computations for Thermal Radiation in MHD Channel Flow with Heat and Mass Transfer", Plos One, **vol. 9**, :e86695. doi:10.1371/ journal.pone.0086695

[2] *J. Hartmann,* "Hg-Dynamics-I", Math-Fys. Medd., **vol. 6**, 1937, pp. 1-28

[3] *I.J. Uwanta, M. Sani and M.O. Ibrahim,* "MHD Convection Slip Fluid Flow with Radiation and Heat Deposition in a Channel in a Porous Medium", International Journal of Computer Applications, **vol. 36**, 2011, pp. 41-48

[4] *M.A. Rashdan, S. M. Fayyad and M. Frihat*, "Heat and mass fully developed natural convective viscous flow with chemical reaction in porous medium", Adv. theor. appl. mech., **vol. 5**, 2012, pp. 93-112
[5] *N. Bachok, A. Ishak and I. Pop*, "Stagnation-point flow over a stretching/shrinking sheet in a nanofluid", Nanoscale Research Letters, **vol. 6**, 2011, pp. 623
[6] *B.S. Bhadauria and P. Kiran*, "Chaotic and oscillatory magneto-convection in a binary viscoelastic fluid under g-jitter", International Journal of Heat and Mass Transfer, **vol. 84**, 2015, pp. 610-624
[7] *S. Abbasbandy, R. Naz, T. Hayat and A. Alsaedi*, "Numerical and analytical solutions for Falkner–Skan flow of MHD Maxwell fluid", Applied Mathematics and Computation, **vol. 242**, 2014, pp. 569-575
[8] *V. Khandelwal, A. Dhiman and L. Baranyi*, "Laminar flow of non-Newtonian shear-thinning fluids in a T-channel", Computers & Fluids, **vol. 108**, 2015, pp. 79-91
[9] *J.W. Hoyt and A.G. Fabula*, The effect of additives on fluid friction, U. S. Naval Ordinance Test Station Report, 1964
[10] *A.C. Eringen*, "Simple Microfluids", Int. J. Eng. Sci., **vol. 2**, 1964, pp. 205-217
[11] *A.C. Eringen*, "Theory of Micropolar Fluids", Journal of Mathematics and Mechanics, **vol. 16**, 1966, pp. 1-18
[12] *C.Y. Cheng*, "Fully developed natural convection heat and mass transfer of a micropolar fluid in a vertical channel with asymmetric wall temperatures and concentrations", International Communications in Heat and Mass Transfer, **vol. 33**, 2006, pp. 627–635
[13] *M. Ahraf, M.A. Kamal and K.S. Syed*, "Numerical simulation of flow of micropolar fluids in a channel with a porous wall", International Journal for Numerical Methods in Fluids, **vol. 66** 2011, pp. 906–918
[14] M. *Ahraf, M.A. Kamal and K.S. Syed*, "Numerical simulation of a micropolar fluid between a porous disk and a non-porous disk", Journal of Applied Mathematics and Modelling, **vol. 33** 2009, pp. 1933-1943.
[15] *M. Ashraf and K. Batool*, "MHD flow and heat transfer of a micropolar fluid over a stretchable disk", Journal of Theoretical and Applied Mechanics, **vol. 51**, 2013, pp. 25-38
[16] *Y. Shangjun, Z. Kequn and W. Wang*, "Laminar flow of micropolar fluid in rectangular microchannels", Acta Mechanica Sinica, **vol. 22**, 2006, pp. 403-408
[17] *M.F. Naccache and P.R. Souza*, "Heat transfer to non-Newtonian fluids in laminar flow through rectangular ducts", International Journal of Thermal Sciences, **vol. 8**, 2011, pp. 16-25
[18] *N.A. Kelson, A. Desseaux and T.W. Farrell*, "Micropolar flow in a porous channel with high mass transfer", ANZIAM, **vol. 44**, 2003, pp. 479-495
[19] *K. Ali, S. Ahmad and M. Ashraf*, "Numerical simulation of MHD pulsatile flow of a biofluid in a channel", AIP Advances, **vol. 5**, **087130,** 2015; http://dx.doi.org/10.1063/1.4928574
[20] *P.J. Roache and P.M. Knupp*, "Completed Richardson Extrapolation", Communications in Numerical Methods in Engineering, **vol. 9**, 1993, pp. 365-374
[21] *P. Deuflhard*, "Order and Step-size Control in Extrapolation Methods", Numerical Mathematics, **vol. 41**, 1983, pp. 399-422
[22] *K. Ali, M. Ashraf and N. Jameel*, "Numerical simulation of magnetohydrodynamic micropolar fluid flow and heat transfer in a channel with shrinking walls", Canadian Journal of Physics (Canada), **vol. 92**, 2014, pp. 987-996
[23] *K. Ali, S. Ahmad, and M. Ashraf*, "On combined effect of thermal radiation and viscous dissipation in hydromagnetic micropolar fluid flow between two stretchable disks", Thermal Science (Serbia), doi: 10.2298/TSC1150325096A (2015).